

# Zeeman quantum beats of helium Rydberg states excited by synchrotron radiation

Yasumasa Hikosaka,<sup>a\*</sup> Hiroshi Iwayama<sup>b</sup> and Tatsuo Kaneyasu<sup>c</sup>

<sup>a</sup>Institute of Liberal Arts and Sciences, University of Toyama, Toyama 930-0194, Japan, <sup>b</sup>Institute for Molecular Science, Okazaki 444-8585, Japan, and <sup>c</sup>SAGA Light Source, Tosu 841-0005, Japan.

\*Correspondence e-mail: hikosaka@las.u-toyama.ac.jp

Received 4 October 2019

Accepted 28 February 2020

Edited by S. Svensson, Uppsala University, Sweden

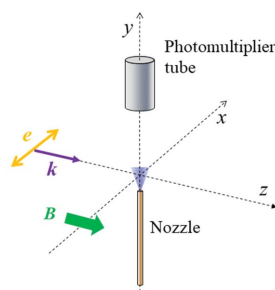
**Keywords:** Zeeman quantum beat; fluorescence; polarization.

Quantum beats in fluorescence decay from Zeeman-split magnetic sublevels have been measured for helium Rydberg states excited by synchrotron radiation. The Zeeman quantum beats observed in this prototypical case were fitted with an equation from a theoretical formulation. It is proposed that Zeeman quantum beat measurement can be a useful way to simply evaluate the polarization characteristics of extreme ultraviolet light.

## 1. Introduction

Increasing numbers of synchrotron radiation experiments in the wavelength range from the extreme ultraviolet (XUV) to soft X-rays utilize the properties of light polarization. A method for evaluating the polarization characteristics of incident light in this range is therefore an important concern in the synchrotron community. The diagnosis of the polarization state can be precisely made with an optical method using polarimeters (Gaupp & Mast, 1989; Koide *et al.*, 1991, 1993; Schäfers *et al.*, 1999; Finetti *et al.*, 2004; Nahon & Alcaraz, 2004). Such a measurement, however, requires stringent alignment of the polarimeters, and the fabrication and manipulation of an effective polarimeter system are still challenging. To avoid these difficulties, it has been proposed that the polarization characteristics of the excitation XUV light be evaluated by observing that of the UV/visible light transformed using atomic resonance (Bobashev & Vasyutinskii, 1992). The experimental feasibility of this method has been investigated (Latimer *et al.*, 1999), but a practical use of this method has not appeared yet.

Compared with optical methods using polarimeters, observation of a material process responding to light polarization generally has an advantage in terms of ease of measurement, in addition to significant cost merit. The linear polarization degree of XUV light can be simply estimated by observing the photoelectron angular distribution of gas samples with a known asymmetry parameter (Houlgate *et al.*, 1974; Krause *et al.*, 1981; Derenbach *et al.*, 1983). This method has been recently applied to shot-to-shot polarization diagnostics of free-electron laser pulses (Allaria *et al.*, 2014; Ferrari *et al.*, 2015; Laksman *et al.*, 2019). In the meantime, all Stokes parameters for soft X-ray light can be determined when angle-resolved photoelectrons are observed in coincidence with angle-resolved Auger electrons (Lörch *et al.*, 1999). Another coincidence method to determine all Stokes parameters is the vector correlation measurement of photoelectrons and fragment ions produced by dissociative photoionization of simple molecules, which can take place over XUV to X-ray wavelengths (Veyrinas *et al.*, 2013).



In this paper, we propose a new method to evaluate the linear polarization of monochromated synchrotron radiation in the XUV range. This method relies on observing quantum beats, which are intensity modulations superposed on the decay curve of fluorescence from coherently excited quantum levels. The frequency of the time modulation corresponds to the energy difference between the coherently excited levels. So far, the observation of quantum beats has usually been utilized in high-resolution spectroscopy of the excited levels in atoms and molecules (Haroche, 1976; Aleksandrov, 1964; Dodd *et al.*, 1964; Hadeishi & Nierenberg, 1965; Andrä, 1970; Bitto & Huber, 1990; Hack & Huber, 1991; Carter & Huber, 2000). A tunable pulsed laser is the standard excitation source in the current quantum beat measurements (Bitto & Huber, 1990; Hack & Huber, 1991; Carter & Huber, 2000). In contrast, although synchrotron radiation of a continuous spectrum extending as far as the hard X-ray range can be a useful excitation source for quantum beat measurements, reports on quantum beat measurement using synchrotron radiation are limited only to Stark-split Rydberg states in Ar (Morioka *et al.*, 2001; Aoto *et al.*, 2005).

Quantum beats in fluorescence decay from Zeeman-split magnetic sublevels of He Rydberg states were observed in this work by excitation with synchrotron radiation. To the best of our knowledge, this prototypical case of quantum beats has not been hitherto investigated, probably because such excitation states lying in the XUV range cannot be easily targeted with lasers. It is shown that the Zeeman quantum beats are well described by a theoretical formulation, and the fitting to the observed quantum beats provides information on the linear polarization degree of the exciting XUV light.

## 2. Experiment

The experiments were carried out at the bending-magnet beamline BL5B of the UVSOR synchrotron facility. The single-bunch operation of the storage ring provided light pulses with a 178 ns repetition period. The duration of the light pulses, resulting from the natural bunch length of relativistic electrons in the storage ring, was 0.3 ns (FWHM). The beamline was equipped with a plane-grating monochromator (Sakurai *et al.*, 1989), and an 800 lines  $\text{mm}^{-1}$  grating was employed in the present measurements. The acceptance angle of the synchrotron radiation by this beamline was  $\pm 2.0$  mrad in the vertical direction and 10 mrad in the horizontal direction. Because of the symmetric acceptance with respect to the storage ring plane, the collected light beam includes right- and left-elliptical polarization components in comparable amounts. This kind of light can be regarded in its practical use as horizontally polarized light with a certain polarization degree. The polarization degree of the partially polarized light is defined as  $P = (I_x - I_y)/(I_x + I_y)$ , where light intensities in the horizontal and vertical directions are  $I_x$  and  $I_y$ , respectively. The polarization degree on the acceptance of this beamline was calculated, using the *SPECTRA* 10.0 program (Tanaka & Kitamura, 2001), to be  $P = 0.74$  at 24 eV light. It is estimated with the X-ray reflectivity data (Henke *et al.*, 1993) that the

beamline optics improves the polarization degree to around  $P = 0.84$ , due to the difference in reflectivity of the optics about *s*- and *p*-polarized light. The actual polarization degree is sensitive to the beamline setting about the vertical acceptance, and it was observed at this beamline that an a-few-mm misalignment of the centre of the vertical acceptance reduces the polarization degree significantly (Hatano *et al.*, 2002).

The monochromated synchrotron radiation was focused by a toroidal mirror and selected by a four-jaw slit whose opening is 1 mm (horizontal)  $\times$  0.5 mm (vertical). Helium gas in the form of an effusive beam crossed the monochromated synchrotron radiation at right angles. The effective gas pressure at the interaction region was maintained below  $2 \times 10^{-3}$  Pa. The effect from radiation re-absorption was sufficiently suppressed in this condition, while attenuation of incident light ( $\sim 40\%$  at the  $n = 3$  resonance energy and  $\sim 20\%$  at the  $n = 4$  resonance energy) is anticipated due to the long incidence path ( $\sim 200$  mm) through the gas. The geometry for observing fluorescence from He is drawn in Fig. 1(a). Fluorescence photons were detected over an acceptance solid angle of about 0.25 sterad, by a photomultiplier tube (Hamamatsu, R6249P) located at right angles to both the polarization and propagation of the monochromated synchrotron light. The photomultiplier tube is sensitive in the wavelength range 300–650 nm and outputs signals of 4.0 ns rise time. The signals from the photomultiplier were converted with a constant-fraction discriminator (ORTEC 584) to NIM signals. The time intervals

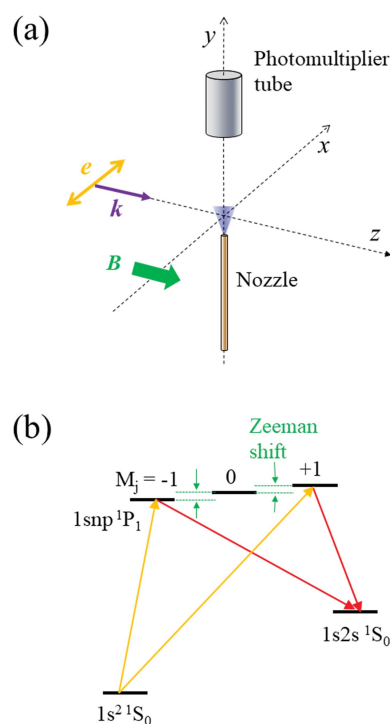


**Figure 1**  
(a) Geometry for observing fluorescence from helium Rydberg states excited by linearly polarized XUV light. (b) Energy level diagram of helium, depicting the excitation and decay pathways relevant to the present measurement.

between the NIM signals and the master clock signal for the storage ring operation were measured by a time-to-amplitude converter (ORTEC 567).

### 3. Results and discussion

Fluorescence yields measured as a function of excitation photon energy are plotted in Fig. 2. Peaks are observed at  $1s \rightarrow np$  excitation energies. The fluorescence photons detected are emitted on the  $np \rightarrow 2s$  decays. The excitation and decay pathways are depicted in Fig. 1(b). The relative peak intensities in Fig. 2, differing from the ones expected by the transition probabilities from the ground state to the Rydberg states (Kramida *et al.*, 2018) and the branching ratios for the  $np \rightarrow 2s$  decays (Theodosiou, 1987), are affected by the detector sensitivity depending on fluorescence wavelength and the incident-light attenuation being more pronounced at lower- $n$  resonances. The peak widths in this spectrum reflect the photon bandwidth of  $\sim 50$  meV (FWHM), and the Rydberg states of  $n < 6$  are well resolved in this setting.

The fluorescence decay curve measured at the photon energy for the  $1s \rightarrow 5p$  excitation is plotted in Fig. 3(a). The decay curve presents a simple exponential decay form and was fitted with the exponential decay function convoluted with a Gaussian function, where the decay lifetime was fixed to the natural lifetime (7.7 ns; Žitnik *et al.*, 2003) of the Rydberg state. The best fit was obtained with a Gaussian width of 2.9 ns (FWHM). This width is attributed to the temporal resolution of the measurement, limited mainly by the slow rise time of the photomultiplier tube output.

To induce quantum beats in the fluorescence decay from the Rydberg state, a magnetic field was applied along the light propagation axis [see Fig. 1(a)], using a pair of solenoid coils placed across the interaction region. The quantization axis ( $z$ -axis) was thus set to be parallel to the light propagation, and the  $M_j = \pm 1$  magnetic sublevels of individual  $np$  Rydberg states could be excited by the linearly polarized light. The magnetic field induces Zeeman shifts of the magnetic sublevels

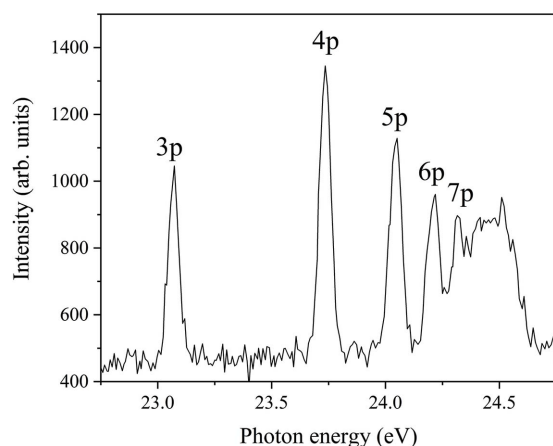


**Figure 2** Fluorescence yield curve measured as a function of excitation photon energy. The detected fluorescence photons are emitted on the  $np \rightarrow 2s$  transitions.

of each  $np$  Rydberg state, as depicted in Fig. 1(b). In a given magnetic field  $B$ , the  $M_j = \pm 1$  levels split with  $\Delta E = 2 \mu_B B$  in energy, where  $\mu_B$  is the Bohr magneton. For instance, an application of a 10 mT magnetic field leads to an energy splitting of 1.2  $\mu\text{eV}$  for the sublevels. Discrimination of such a tiny splitting is far beyond the resolution of current XUV frequency-domain spectroscopy using a synchrotron light source. Assuming a Fourier-transform-limited light pulse, the temporal width should be shorter than 0.55 ns to excite these Zeeman levels coherently. Indeed, the pulse duration of the present study meets the requirement. In practice, the light pulse of synchrotron radiation is by no means Fourier-transform-limited light, and obviously these states are excited coherently. On the contrary, considering that the emission from every single relativistic electron has a wide spectrum ranging from infrared to X-ray, in theory the synchrotron light pulses would give rise to coherent excitation to states separated by hundreds of eV. Coherent excitation by undulator radiation to Rydberg states lying in an a-few-eV range was recently proved in the observation of interferences between the Rydberg wave packets launched by the excitation (Hikosaka *et al.*, 2019).

Fluorescence decay curves at the  $1s \rightarrow 5p$  excitation, measured at three different magnetic field strengths, are presented in Figs. 3(b)–3(d). Unlike the decay curve in Fig. 3(a), these curves exhibit quantum beat oscillations superposed on the exponential-decay form. This observation

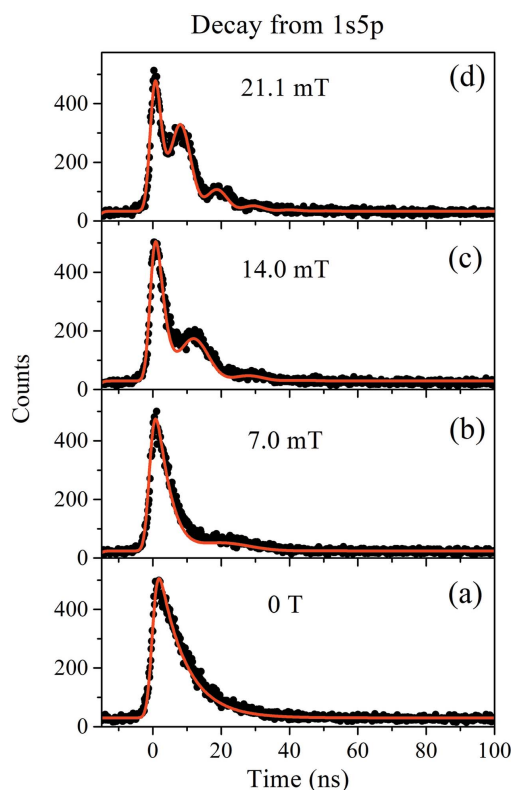


**Figure 3** Fluorescence decay curves (dots) of the  $1s5p$  excited state in helium, measured with different magnetic fields. Each curve was obtained by an accumulation of around 10 min. The red solid curves are the best fits to the observations (see text).

manifests the coherent excitation to the Zeeman-split  $M_j = \pm 1$  levels. The oscillation frequency of the quantum beat increases with the increase in magnetic field, due to the larger level splitting at higher magnetic field strength. In the meantime, the quantum beat structure completely vanished when the direction of the magnetic field was switched to be parallel to the electric vector (not shown), where the excitation to the  $M_j = 0$  level is solely allowed.

The theoretical formulation of the Zeeman quantum beat of an  $np$  Rydberg state in He can be given as follows. The time evolution of the superposition state prepared by linearly polarized light can be written as

$$|\psi(t)\rangle = \frac{1}{\sqrt{2}} \left[ \langle +1|\mu_{XUV}|1s\rangle \exp(-i\omega_+t - \gamma t/2)|+1\rangle + \langle -1|\mu_{XUV}|1s\rangle \exp(-i\omega_-t - \gamma t/2)|-1\rangle \right], \quad (1)$$

where  $\langle +1|\mu_{XUV}|1s\rangle$  and  $\langle -1|\mu_{XUV}|1s\rangle$  are the transition dipole moments from the ground state  $|1s\rangle$  to the magnetic sublevels  $|+1\rangle$  and  $|-1\rangle$  of the  $np$  Rydberg state, respectively.  $\omega_+$  and  $\omega_-$  are the respective transition frequencies, and  $\gamma$  is the decay constant common to the magnetic sublevels (Carter & Huber, 2000). The fluorescence intensity in the decay of the superposition state  $|\psi(t)\rangle$  into the final state  $|2s\rangle$  is proportional to the square of the transition matrix element of the fluorescence transition,

$$I(t) \propto |2s|\mu_{UV}|\psi(t)|^2. \quad (2)$$

After substituting equation (1) into equation (2), the latter can be written as

$$I(t) \propto |2s|\mu_{UV}|+1\rangle\langle +1|\mu_{XUV}|1s\rangle \exp(-i\omega_+t - \gamma t/2)|+1\rangle + |2s|\mu_{UV}|-1\rangle\langle -1|\mu_{XUV}|1s\rangle \exp(-i\omega_-t - \gamma t/2)|-1\rangle|^2. \quad (3)$$

Since the transition moments about the two magnetic sublevels are equal in magnitude, the time evolution of the fluorescence intensity monitored at a particular direction  $\phi$  with respect to the polarization direction of light can be simplified as (Carter & Huber, 2000)

$$I(t) \propto [1 + \cos(\Delta\omega t + 2\phi)] \exp(-\gamma t), \quad (4)$$

where  $\Delta\omega = \omega_+ - \omega_-$ . For the partially polarized light whose light intensities in the horizontal and vertical directions are  $I_x$  and  $I_y$ , respectively, the fluorescence intensity monitored at an angle  $\phi$  from the vertical direction can be given as

$$I(t) \propto \left[ I_x + I_x \cos(\Delta\omega t + 2\phi) + I_y + I_y \cos(\Delta\omega t + 2\phi + \pi) \right] \times \exp(-\gamma t). \quad (5)$$

Using polarization degree of  $P = (I_x - I_y)/(I_x + I_y)$ , equation (5) can be simplified as

$$I(t) \propto [1 + P \cos(\Delta\omega t + 2\phi)] \exp(-\gamma t). \quad (6)$$

Equation (6) indicates that modulation of the frequency  $\Delta\omega$  superposes on the exponential decay function observed in an ordinary exponential decay, where the visibility of the oscil-

lation reflects the degree of light polarization. Here, the phase of the quantum beat oscillation depends on  $\phi$  and thus implies the polarization direction with respect to the detection direction.

The quantum beats observed essentially result from the integration over the solid angle of the fluorescence observation. The integration of equation (6) over a range from  $\phi = -\Phi$  to  $\phi = +\Phi$  gives

$$I(t) \propto [1 + P_{\text{obs}} \cos \Delta\omega t] \exp(-\gamma t), \quad (7)$$

where  $P_{\text{obs}} = (P \sin 2\Phi)/2\Phi$ . Equation (7) was applied to fit the decay curves in Figs. 3(b)–3(d). Prior to the fittings, the  $\Delta\omega$  values of the quantum beats were determined by Fourier-transform analysis of the decay curves. The effective magnetic fields in the interaction region, indicated in these figures, were deduced from the determined  $\Delta\omega$  values. Fitting with equation (7) to each decay curve was implemented as follows, without deriving the complicated analytic expression of equation (7) convoluted with the temporal resolution of the measurement. For a particular  $P_{\text{obs}}$  value, equation (7) was numerically convoluted with a Gauss function (FWHM of 2.9 ns) and the minimum residual to the observed curve was searched by varying the scaling factor and the baseline. This procedure was repeated for different  $P_{\text{obs}}$  values and the best fit was pursued. The best fits thus obtained for the three decay curves are presented in the figures with solid curves. The fitting provides  $P_{\text{obs}} = 0.60 \pm 0.05$ , where the error was estimated from the differences among the values obtained from the three different curves. Considering the relation  $P_{\text{obs}} = (P \sin 2\Phi)/2\Phi$ , the polarization degree of the excitation light is at least better than  $0.60 \pm 0.05$ .

The angular range for the fluorescence observation reflects the detection solid angle and the source volume. The angular range of the present observation is effectively around  $\Phi = 0.35$  rad, although it is an approximation considering the circular detection area of the photomultiplier and the entrance of fluorescence from out of the  $x$ - $y$  plane defined in Fig. 1(a). With this  $\Phi$  value, the polarization degree can be determined to be around  $P = 0.65$ . This value is rather small compared with the ideal value ( $P = 0.84$ ) estimated from the acceptance angle of the beamline and the reflectivity of the beamline optics. Separate measurement of the actual polarization degree will be useful to evaluate the accuracy of the present measurement, considering that the polarization degree is subject to easy reduction depending on the beamline setting (Hatano *et al.*, 2002). The large detection solid angle and the large source volume of the present measurement may bring a sizable error in the estimation of the effective angular range and thus in the determined polarization degree. In addition, inhomogeneity of the magnetic field in the large source volume can reduce the measured value. In these respects, a more accurate estimation of the polarization degree can be made by observing fluorescence with a smaller detection solid angle, which is fully feasible considering the favourable count rates in the present investigations (each spectrum in Fig. 3 was obtained by a 10 min accumulation).

Fig. 4 compares the quantum beats in the fluorescence decay curves measured for three different Rydberg states in He. The magnetic field was fixed at 21.1 mT in these measurements. While the decay curves of higher Rydberg states show longer lifetimes, a common beat frequency is observed due to the application of the identical magnetic field. The degrees of the light polarization at these photon energies were investigated by the fitting procedure described above, and no essential difference was detected at these adjacent photon energies.

In conclusion, we have observed Zeeman quantum beats of Rydberg states in He, with monochromated synchrotron radiation. The observed quantum beats were well fitted with the established formulation, and the polarization degree was estimated from the fittings. The present work shows the capability of Zeeman quantum beat observation to simply evaluate the linear polarization of XUV light. Angle-resolved photoelectron spectroscopy is currently the most popular way to determine the linear polarization of light in the XUV and soft X-ray ranges. On the other hand, the applicable photon energies of Zeeman beat measurement are limited to the XUV range, where resonance states with long decay lifetimes lie. However, this new method has advantages in its simpler setup and easier operation, as it can be implemented with a single suitable photomultiplier placed out of vacuum. In practical use, it is convenient that Zeeman beat measurement can be conducted under a low vacuum condition. Another useful property is that the polarization direction can be readily determined by the phase of the quantum beat oscillation. In practice, we currently utilize this property in investigating the spatial distribution of polarization direction in an XUV vector beam (Matsuba *et al.*, 2018) produced by a crossed undulator

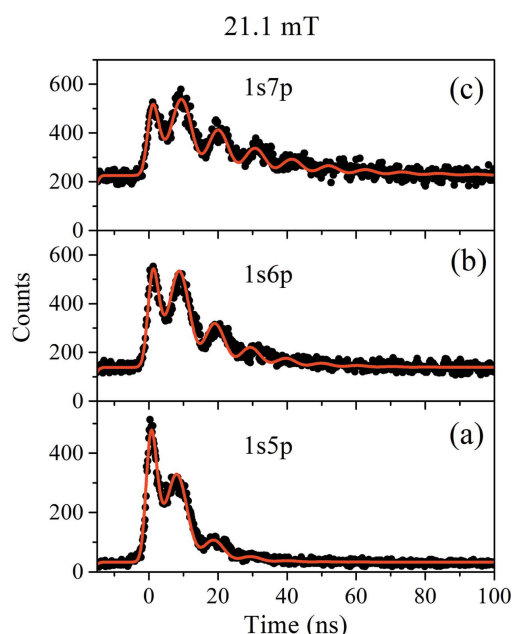


**Figure 4** Fluorescence decay curves (dots) measured at the resonances of  $1s5p$ ,  $1s6p$  and  $1s7p$ . The magnetic field was fixed at 21.1 mT in these measurements. The red solid curves are the best fits to the observations (see text). The curves in (a) are replots of those in Fig. 3(d).

setup. In these respects, Zeeman beat measurement can be a useful new option to evaluate the linear polarization of XUV light.

### Acknowledgements

The experiments were performed at the UVSOR synchrotron facility (proposal Nos. 2017-574 and 2017-851). We are grateful to the UVSOR staff for the stable operation of the synchrotron ring. This work was partly supported by Matsuo Foundation and Research Foundation for Opto-Science and Technology.

### Funding information

The following funding is acknowledged: Matsuo Foundation; Research Foundation for Opto-Science and Technology.

### References

- Aleksandrov, E. B. (1964). *Opt. Spectrosc.* **17**, 522 (Engl. Transl.).
- Allaria, E., Diviacco, B., Callegari, C., Finetti, P., Mahieu, B., Viehhaus, J., Zangrando, M., De Ninno, G., Lambert, G., Ferrari, E., Buck, J., Ilchen, M., Vodungbo, B., Mahne, N., Svetina, C., Spezzani, C., Di Mitri, S., Penco, G., Trovó, M., Fawley, W. M., Rebernik, P. R., Gauthier, D., Grazioli, C., Coreno, M., Ressel, B., Kivimäki, A., Mazza, T., Glaser, L., Scholz, F., Seltmann, J., Gessler, P., Grünert, J., De Fanis, A., Meyer, M., Knie, A., Moeller, S. P., Raimondi, L., Capotondi, F., Pedersoli, E., Plekan, O., Danailov, M. B., Demidovich, A., Nikolov, I., Abrami, A., Gautier, J., Lüning, J., Zeitoun, P. & Giannessi, L. (2014). *Phys. Rev. X*, **4**, 041040.
- Andrá, H. J. (1970). *Phys. Rev. Lett.* **25**, 325–327.
- Aoto, T., Sakakida, I., Yoshii, H., Hayaishi, T. & Morioka, Y. (2005). *J. Electron Spectrosc. Relat. Phenom.* **144–147**, 47–50.
- Bitto, H. & Robert Huber, J. (1990). *Opt. Commun.* **80**, 184–198.
- Bobashev, V. & Vasyutinskii, O. S. (1992). *Rev. Sci. Instrum.* **63**, 1509.
- Carter, R. T. & Huber, J. R. (2000). *Chem. Soc. Rev.* **29**, 305–314.
- Derenbach, H., Malutzki, R. & Schmidt, V. (1983). *Nucl. Instrum. Methods Phys. Res.* **208**, 845–847.
- Dodd, J. N., Kaul, R. D. & Warrington, D. M. (1964). *Proc. Phys. Soc.* **84**, 176–178.
- Ferrari, E., Allaria, E., Buck, J., De Ninno, G., Diviacco, B., Gauthier, D., Giannessi, L., Glaser, L., Huang, Z., Ilchen, M., Lambert, G., Lutman, A. A., Mahieu, B., Penco, G., Spezzani, C. & Viehhaus, J. (2015). *Sci. Rep.* **5**, 13531.
- Finetti, P., Holland, D. M. P., Latimer, C. J. & Binns, C. (2004). *Nucl. Instrum. Methods Phys. Res. B*, **215**, 565–576.
- Gaupp, A. & Mast, M. (1989). *Rev. Sci. Instrum.* **60**, 2213–2215.
- Hack, E. & Huber, J. R. (1991). *Int. Rev. Phys. Chem.* **10**, 287–317.
- Hadeishi, T. & Nierenberg, G. A. (1965). *Phys. Rev. Lett.* **14**, 891–892.
- Haroche, S. (1976). In *High-Resolution Laser Spectroscopy*, edited by K. Shimoda. Berlin: Springer.
- Hatano, T., Kondo, Y., Saito, K., Ejima, T., Watanabe, M. & Takahashi, M. (2002). *Surf. Rev. Lett.* **09**, 587–591.
- Henke, B. L., Gullikson, E. M. & Davis, J. C. (1993). *At. Data Nucl. Data Tables*, **54**, 181–342.
- Hikosaka, Y., Kaneyasu, T., Fujimoto, M., Iwayama, H. & Katoh, M. (2019). *Nat. Commun.* **10**, 4988.
- Houlgate, R. G., Codling, K., Marr, G. V. & West, J. B. (1974). *J. Phys. B: At. Mol. Phys.* **7**, L470–L473.
- Koide, T., Shidara, T. & Yuri, M. (1993). *Nucl. Instrum. Methods Phys. Res. A*, **336**, 368–372.
- Koide, T., Shidara, T., Yuri, M., Kandaka, N., Yamaguchi, K. & Fukutani, H. (1991). *Nucl. Instrum. Methods Phys. Res. A*, **308**, 635–644.

- Kramida, A., Ralchenko, Yu., Reader, J. & NIST ASD Team (2018). *NIST Atomic Spectra Database* (Version 5.6.1) [Online]. Available at <https://physics.nist.gov/asd> [24 July 2019]. National Institute of Standards and Technology, Gaithersburg, MD, USA. <https://doi.org/10.18434/T4W30F>.
- Krause, M. O., Carlson, T. A. & Woodruff, P. R. (1981). *Phys. Rev. A*, **24**, 1374–1379.
- Laksman, J., Buck, J., Glaser, L., Planas, M., Dietrich, F., Liu, J., Maltezopoulos, T., Scholz, F., Seltmann, J., Hartmann, G., Ilchen, M., Freund, W., Kujala, N., Viefhaus, J. & Grünert, J. (2019). *J. Synchrotron Rad.* **26**, 1010–1016.
- Latimer, C. J., MacDonald, M. A. & Finetti, P. (1999). *J. Electron Spectrosc. Relat. Phenom.* **101–103**, 875–878.
- Lörch, H., Scherer, N., Kerkau, T. & Schmidt, V. (1999). *J. Phys. B At. Mol. Opt. Phys.* **32**, L371–L379.
- Matsuba, S., Kawase, K., Miyamoto, A., Sasaki, S., Fujimoto, M., Konomi, T., Yamamoto, N., Hosaka, M. & Katoh, M. (2018). *Appl. Phys. Lett.* **113**, 021106.
- Morioka, Y., Aoto, T. & Yoshii, H. (2001). *Phys. Rev. A*, **64**, 053409.
- Nahon, L. & Alcaraz, C. (2004). *Appl. Opt.* **43**, 1024–1037.
- Theodosiou, C. E. (1987). *At. Data Nucl. Data Tables*, **36**, 97–127.
- Sakurai, M., Morita, S., Fujita, J., Yonezu, H., Fukui, K., Sakai, K., Nakamura, E., Watanabe, M., Ishiguro, E. & Yamashita, K. (1989). *Rev. Sci. Instrum.* **60**, 2089–2092.
- Schäfers, F., Mertins, H. C., Gaupp, A., Gudat, W., Mertin, M., Packe, I., Schmolla, F., Di Fonzo, S., Soullié, G., Jark, W., Walker, R., Le Cann, X., Nyholm, R. & Eriksson, M. (1999). *Appl. Opt.* **38**, 4074–4088.
- Tanaka, T. & Kitamura, H. (2001). *J. Synchrotron Rad.* **8**, 1221–1228.
- Veyrinas, K., Elkharrat, C., Marggi Poullain, S., Saquet, N., Doweck, D., Lucchese, R. R., Garcia, G. A. & Nahon, L. (2013). *Phys. Rev. A*, **88**, 063411.
- Žitnik, M., Stanič, A., Bu ar, K., Lambourne, J. G., Penent, F., Hall, R. I. & Lablanquie, P. (2003). *J. Phys. B At. Mol. Opt. Phys.* **36**, 4175–4189.